Fuelling and density control for DEMO

P Vincenzi[1,2,*], F Koechl[3], L Garzotti[4], D B King[4], E Tindale[4], T Bolzonella[1], P T Lang[5], B Pegourié[6], M Romanelli[4] and R Wenninger[5,7]

[1]Consorzio RFX (CNR, ENEA, INFN, Università di Padova, Acciaierie Venete SpA) Corso Stati Uniti 4 - 35127 Padova, Italy
[2]Università degli Studi di Padova, 35122 Padova, Italy
[3]Association EURATOM-ÖAW/ATI, Atominstitut, TU Wien, Austria
[4]CCFE, Culham Science Centre, Abingdon OX14 3DB, UK
[5]Max-Planck-Institut fur Plasmaphysik, EURATOM-Association, D-85748, Garching, Germany
[6]CEA/IRFM, 13108 St Paul-lez-Durance, France
[7] EUROFusion, Programme Management Unit, 85748 Garching, Germany

*Corresponding author. Tel.: +39.049.829.5000/1; fax: +39.049.8700718.
E-mail address: pietro.vincenzi@igi.cnr.it (PV).

Abstract. Plasma fuelling and density control are an open issue regarding EU DEMO studies and solutions may be different from present day experiments. The present paper addresses through JINTRAC core transport code simulations the feasibility of different fuelling methods as gas puff and pellet injection and the influence of neoclassical and anomalous inward pinch in the edge transport barrier in order to achieve and control the target DEMO density. Given the expected high fusion power production, He accumulation in the plasma core is a critical issue, and an estimation of the influence of impurities (He, Ar and W) on core fuelling and plasma dilution is given together with a discussion on D-T core balance. The DEMO reference scenario investigated in this work is characterized by a peaked density profile, which requires a careful core fuelling. Due to the large pedestal temperature gradient, gas puff may not be a feasible option for core density control, unless assuming a large anomalous inwards pinch in the edge transport barrier of more than ~2 m/s. Pellet injection from high field side of the torus, on the contrary, may represent a viable solution for core fuelling and D-T ratio control. The effect of pellet mass, speed and injection geometry is also discussed in the present paper. Regardless, core fuelling efficiency with pellet injection is almost entirely determined by the presence of $\boldsymbol{E}$x$\boldsymbol{B}$ drift.

1. Introduction

According to the EU fusion roadmap Horizon 2020 [1], the next step beyond ITER in the path towards commercial fusion power plants is planned to be a Demonstration Fusion Power Reactor (DEMO). R&D towards a conceptual design for EU DEMO is an ongoing process, addressing both engineering and physics issues. Great experience is expected to be gained from ITER construction and operation, with consequent contributions to DEMO development.

Density control and plasma fuelling are key topics for the design of DEMO, and only few studies are available in literature: an investigation on pellet injection requirements for a helical fusion reactor is illustrated for instance in reference [2]. The approach for particle fuelling may be different from present day tokamaks and may follow the same method intended for ITER, with a significant core fuelling by pellets injected from the High Field Side (HFS) of the machine [3]. This has not been verified yet, and the present paper tries to shed light, by means of JINRAC core transport code [4] simulations, on feasibility of achieving and controlling the target density of DEMO scenario considering different options. The impurity accumulation issue in the core region is also addressed here.

An efficient plasma fuelling must ensure the maintenance of the prescribed density from edge to core: this is a complex matter because of the large plasma volume characterizing a reactor-sized tokamak and the restrictions imposed by the high fusion performances expected. The control of density required for DEMO therefore affects many aspects. Starting from the edge, control of Scrape-Off-Layer (SOL) main ion and impurity densities involves directly power exhaust. It influences the regulation of the divertor power flux and the detachment control. Adequate impurity content in the edge is necessary to guarantee a minimum radiation level, which reduces the power heat flux to plasma facing components [5], [6]. Also, the edge heat

flux must be kept above the L-H power threshold. SOL control is crucial also to avoid imbalance on D-T ratio in the plasma core in case of no pellet fuelling, to reduce the T fraction in proximity to plasma facing components and to prevent plasma core from contamination by W and extrinsic impurities causing degradation in confinement. The control of core main ion density is critical to achieve and maintain a balanced D-T ratio (1:1) and an efficient fusion burn. Moreover He produced by fusion reactions could accumulate reducing fusion performance. Finally scenarios with peaked density profile exceeding the Greenwald limit may require precise central fuelling [7].
Direct actuators for density control are gas puffing, pellet injection, pumping and, for present day experiments, Neutral Beam Injection (NBI). There are of course indirect actuators such as plasma transport and instabilities, which may affect confinement properties, transport barriers and ion collisionality. Peculiar effects have also to be considered, e.g. temperature screening effect (the outward impurity flow caused by the thermal force, see [8]) and pellet induced transport enhancement [9].
This work will discuss the topic of density control and fuelling of DEMO plasma by gas puff or pellet injection (including a discussion on pellet speed, mass and injection trajectories). It will also address the influence of neoclassical and of possible anomalous inward pinch in the Edge Transport Barrier (ETB) and it will estimate criticalities for impurity contamination of the core, He ash accumulation and D-T core balance.
The present paper introduces in section 2 the reference DEMO scenario and simulation assumptions. Then it investigates the effects of different density control actuators by means of numerical simulations in section 3. Effects on core impurity contamination and He ash retention are analysed in subsection 3.1, while gas puffing is discussed in subsection 3.2. Given the probable premature ionization of all (or almost all) D and T particles in the SOL, the requirements on additional anomalous inward pinch in the ETB to sustain DEMO scenario density level are examined in subsection 3.3. In subsection 3.4 the pellet injection option is analysed, and the effect of the plasmoid $\boldsymbol{E}$x$\boldsymbol{B}$ drift on pellet fuelling is discussed in the subsection 3.4.1. Section 4 presents a discussion on the effect of different pellet masses, pellet speeds and injection geometries. The paper ends with conclusions in section 5.

2. DEMO main parameters and simulation conditions

In the present work we analyse the European DEMO tokamak inductive scenario (pulsed scenario), also referred to as DEMO 1 to be distinguished from DEMO 2 which is meant to be a steady state tokamak. DEMO 1 is based on ITER stationary H-mode scenario and aims at achieving more than 1500 MW of fusion power with a pulse length of about 2 hours. DEMO 1 is indeed based on physics and technology presently available (or from a "low extrapolation"), therefore not requiring any critical breakthrough. This concept is intended to be an option which could be delivered in short-medium term. The design of EU DEMO is an ongoing process and parameters are frequently updated: an overview of recent status of design and R&D activities is given in [10] where a scenario with parameters as those used in this work is discussed. Main parameters of DEMO machine are shown in table 1.

Table 1. Global parameters of DEMO 1 inductive scenario used in the present work.

DEMO 1 parameters (pulsed, inductive scenario)	
Major radius, minor radius	9.0 m, 2.45 m
Aspect ratio	3.62
κ_{95}	1.564
δ_{95}	0.333
Plasma volume	1783.0 m^3
Plasma current	16.789 MA
Vacuum B_T at R_0	6.49 T
H factor	1.1

2.1 Simulation conditions

Fully predictive simulations have been carried out with the JINTRAC code suite [4], using the 1.5D transport code JETTO [11] coupled with SANCO code [12] for impurity evolution. ^{4}He, Ar and W impurities have been considered in the simulations, except for simulations in section 4 where Ar is used as only representative impurity: since in section 4 the interest is focused on pellet requirements and not on radiation or power balance, this choice simplifies the simulations in section 4 without influencing the conclusions (see section 4 for further details). Safety factor profile (q), kinetic profiles and impurity density for each ionized

stage (except for W where ionisation stages are represented by groups of contiguous superstages [13]) are typical outputs. SANCO solves the continuity equations for all the ionization stages of the impurities (or "superstages" if bundling scheme is used) together with a continuity equations for neutral impurities. Impurities enter the plasma as neutrals and SANCO code calculates the penetration depth and ionization. Diffusivity is taken into account plus neoclassical convection and anomalous contribution. Boundary conditions on each impurity are imposed prescribing a neutral influx, the wall recycling coefficients and the escape velocity parameter which determines the impurity outflux. The impurity influx from the wall (i.e. impurity outflux times the recycling coefficient) and the additional prescribed neutral influx represent the impurity sources in the plasma. In the simulations shown here the influx from the wall is set to zero by null recycling coefficients and no additional neutral flux. Further details on SANCO sources and sinks can be found in [14]. Plasma boundary is prescribed to a given triangular shape with plasma current I_p of 16.8 MA and a toroidal magnetic field B_0 of 6.5T (values listed in table 1). The equilibrium inside the plasma boundary is solved with the 2D equilibrium solver ESCO [11], considering the pressure contribution from fast alpha and NB particles.

The model assumed for core heat and particle transport is GLF-23 [15] (for anomalous transport) plus NCLASS [16] (for neoclassical contributions) with continuous sawtooth model. Ion and electron heat conductivities, particle diffusivities and convective velocities are self-consistently determined by GLF-23 and NCLASS [17] in all the simulations here presented, except in simulations in section 4 where further details on the model used are given. GLF-23 provides effective diffusivities as output which are interpreted in JINTRAC as diffusivities if they are positive and as convective velocities if they are negative such that the total anomalous flux remains unchanged. In the ETB, anomalous transport is reduced to less than ~0.1% of the values predicted by GLF-23, so that the anomalous contribution becomes negligible in the ETB. In subsection 3.3 "Scan in additional anomalous inward pinch in the ETB" a constant additional anomalous pinch in the ETB of 0.5-2.0 m/s has been applied in the barrier region. Impurity-specific anomalous transport is also determined by GLF-23. GLF-23 model can consider only one main ion and one impurity species at the time. In order to predict the anomalous transport in presence of more than one main ion and impurity species, local averages are calculated for the main ion, the impurity mass and charge numbers and are passed as input to GLF-23. The same diffusivity and pinch velocity predictions from GLF-23 for main ions are then attributed to both D and T, and the same impurity specific diffusivity and pinch velocity predictions are attributed to all impurity species. The edge transport barrier (ETB) is modelled with NCLASS assuming the maximum normalized pressure gradient α_{crit} [18] to be 2.5, and the lower limit of particle diffusivity and heat conductivity of D,χ=0.05 m^2/s. Rather optimistic predictions for the pedestal pressure are obtained with the choice of α_{crit}=2.5. This value has been chosen to reach the target fusion performance of the DEMO scenario presented e.g in [10] and [19]. Accordingly, the pedestal width has been fixed to Δ_{ETB} ~ 12 cm on the outer mid-plane. In the discrete ELMs model applied, small controlled ELMs of 2 MJ are triggered once a critical normalised pressure gradient of α_{crit}=2.5 is exceeded on average in a region that is wider than $\Delta\rho_N$~0.05 in the ETB (where ρ_N is the square root of the normalized toroidal flux). Transport is then strongly increased for the duration of the ELM (automatically adjusted in order to achieve a plasma thermal energy reduction ΔW_{th} of 2 MJ per ELM), applying additional transport with an increase of D and χ centred at r/a=0.98 with Gaussian shape. The assumption of 2 MJ per ELM appears to be appropriate as a conservative estimate with respect to divertor heat load requirements in DEMO, as it can be derived from the estimates in [19]. Auxiliary heating power by NBI is prescribed to 50 MW and injection of 1 MeV D particles is considered by means of the PENCIL code [20]. The time dependent pellet source is modelled by the HPI2 code [21].

Boundary conditions are set to keep an electron density of ~2.5-3.0*10^{19} m^{-3} with a temperature of ~100 eV at the separatrix (cf. expectations for ITER conditions in case of significant impurity seeding [22]) and impurities crossing it with an outward escape velocity of 1 m/s, except for the simulation with reduced escape velocity presented in subsection 3.1 where a value of 0.01 m/s is given for Ar and W impurities (He is still 1 m/s). Neutral influx at the separatrix is prescribed or else set to zero.

The limits of the model assumed in these simulations include the imposed physical parameters at the separatrix and an optimistic assumption on pedestal pressure, although necessary to reach the high fusion performance of DEMO machine. Moreover, when a larger machine is studied by means of models shaped on present-day experiments, some uncertainties might be present since the results rely on extrapolations. This

limit is however intrinsic when we expand our research area to new domains (as already done with ITER design).

2.2 DEMO flattop phase target parameters

A JINTRAC simulation of DEMO flattop phase has been run with the parameters shown in table 1, achieving a fusion power of ~1600 MW. In order to maintain a line-average electron density of ~$8.5*10^{19}$ m^{-3} with density peaking (corresponding to a volume-average density of ~$7.5*10^{19}$ m^{-3}), a feedback control acting on the prescribed neutral influx at the separatrix (equal for D and T) is implemented. Pellets are not used in the simulations before subsection 3.4. Volume-average electron temperature is ~14 keV. Figure 1 shows temperature and density profiles as a function of ρ_N. Although NBI and alpha particles preferentially heat electrons, strong radiation losses make the net heating to ions and electrons comparable in the core region. This explains why the simulation shows $T_i \sim T_e$. Deviation in the D-T ratio of only a few % occurs within a few seconds and remains in stationary conditions. Differences in D and T densities are caused by the D source in the core due to NBI, different average core penetration depth of incoming D and T neutrals, and differences in neoclassical transport predicted by NCLASS model for D and T.

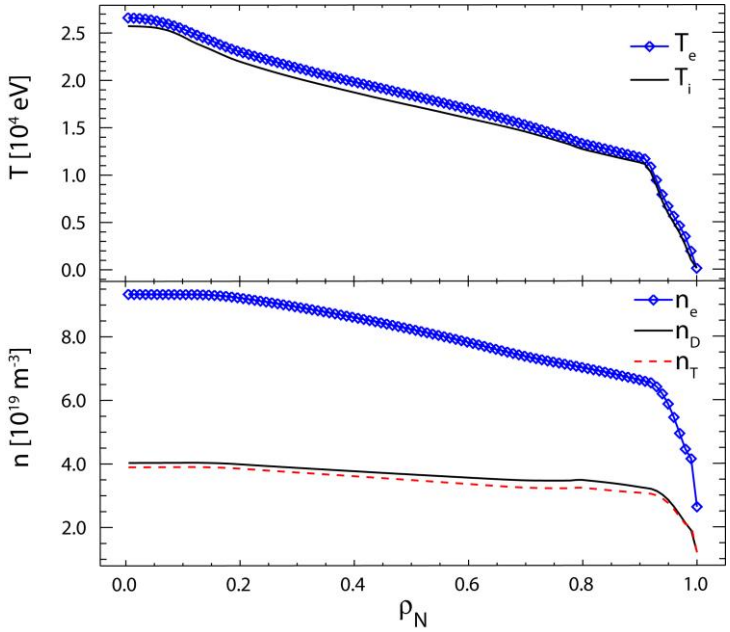

Figure 1. Temperature (top) and density (bottom) profiles of main ions and electrons during typical DEMO flattop phase in stationary conditions.

The DEMO pedestal has a very steep pressure gradient and the temperature at the top of the barrier exceeds 10 keV, reaching 25 keV in the centre, while density at the top of the pedestal is ~$6.5*10^{19}$ m^{-3}. ITER values for the pedestal shows a similar density but lower temperature (around 4 keV) [23]. This means an ITER pedestal pressure roughly half that of DEMO, for which pedestal assumptions seems to be quite optimistic. A recent prediction of DEMO pedestal pressure which has been estimated starting from MHD stability calculations is given in [24], and it suggests a lower pedestal temperature.

The resulting fusion reaction rates in stationary conditions are the following: the reaction rate for thermal D-T is ~$5.5*10^{20}$/s, for beam-thermal D-T ions the reaction rate is ~$6*10^{18}$/s, thermal D+D$\rightarrow{}^3$He+n reaction rate is ~$1.5*10^{18}$/s and beam-thermal D+D$\rightarrow{}^3$He+n reaction rate is ~$4*10^{17}$/s. About 2.2 MW of fusion power are generated only by D+D$\rightarrow{}^3$He+n and D+D$\rightarrow$T+p reactions in the presented simulation. ^{3}He fusion product transport is not solved in the presented simulations.

3. Effect on density control by different actuators

The present work examines different fuelling methods and various effects which can contribute to the achievement and maintenance of the target density for the flattop phase of the DEMO inductive scenario.

Direct fuelling, as gas puff and pellet injection, is examined together with particle transport, as well as the effect of temperature screening of impurities on fuelling conditions and additional inward pinch for D and T.

All the simulations are based on the reference flattop scenario presented in section 2.
Poloidal and toroidal asymmetries in the pellet and neutral sources are not modelled in JETTO transport code. However the pellet code HPI2 does calculate the pellet particle source locally and considers the local variation of the net drift displacement; from this calculation, a flux surface averaged pellet particle source is determined and passed to JETTO.
In present day experiments Neutral Beam Injection (NBI) represents a non-negligible source of particles. Due to the larger plasma volume in machines as ITER or even more as DEMO, NBI systems as those we are considering will have a negligible contribution on plasma fuelling and density control. In DEMO, particle injection from the beams is at least two order of magnitude less compared to other sources, therefore it is not accounted as an actuator for plasma fuelling, although the NB particle source is considered in the modelling.

3.1 Effect of impurities on main ion fuelling and confinement
In current experiments as JET, density peaking seems to facilitate impurity accumulation under certain conditions, while noble gas seeding as Ar seems to be favourable for plasma performance [8]. In DEMO, impurity seeding might be essential to reduce the heat flux to the divertor target plates by impurity induced radiation. Moreover, considering DEMO burning plasma, plasma dilution by He is expected due to the high fusion power. It is thus expected that the core plasma in DEMO will be significantly contaminated by impurities.
In order to evaluate the effect of the impurity contamination of the plasma core on fuelling and confinement conditions, two cases with different boundary conditions on impurity transport have been simulated. The first case has a reduction in the escape velocity of Ar and W impurities to ~0 m/s (0.01 m/s), while the second does not have any reduction in the escape velocities (kept to 1 m/s). The escape velocity is defined as the velocity of these impurities moving towards the SOL. In the present simulation Ar and W losses to the SOL are not compensated. Depending on the imposed escape velocities at the separatrix, the Ar and W impurity content evolves at different time scales. In this way, two different temporary level of impurity concentration of Ar and W are obtained (case 1 with higher and case 2 with lower Ar and W particle content).
Impurity concentration is shown in figure 2 for a period of 4 s, which is of the same order of magnitude of particle confinement time of main ions. While in case 1 the impurity content remains roughly constant, the amount of W and Ar present in the core is reduced to a lower level in case 2. The He core particle content, to the contrary, is quickly increasing due to accumulation of He ash from D-T burn, in both cases (figure 2). High-Z impurity content (i.e. W, as the figure shows) is 3 orders of magnitude less than lower Z impurities. Neoclassical convection in the barrier causes an outwards drift of high Z impurities. It is caused by the large temperature gradient in DEMO (temperature screening effect). Due to ambipolarity and the principle of detailed balance [25], the large neoclassical outflux of high Z impurities is balanced by a neoclassical inwards pinch for low Z impurities and main ions. Quasi-neutrality is indeed enforced both in neo-classical and anomalous transport models. Temperature screening might therefore not only be helpful for the control of core contamination by high Z impurities but also for core fuelling by main ions. In the simulation, the balance of neoclassical fluxes is not affected by anomalous transport, as neoclassical transport is calculated independently with NCLASS model. The influence of turbulent fluctuations on neoclassical transport properties is therefore not taken into account.

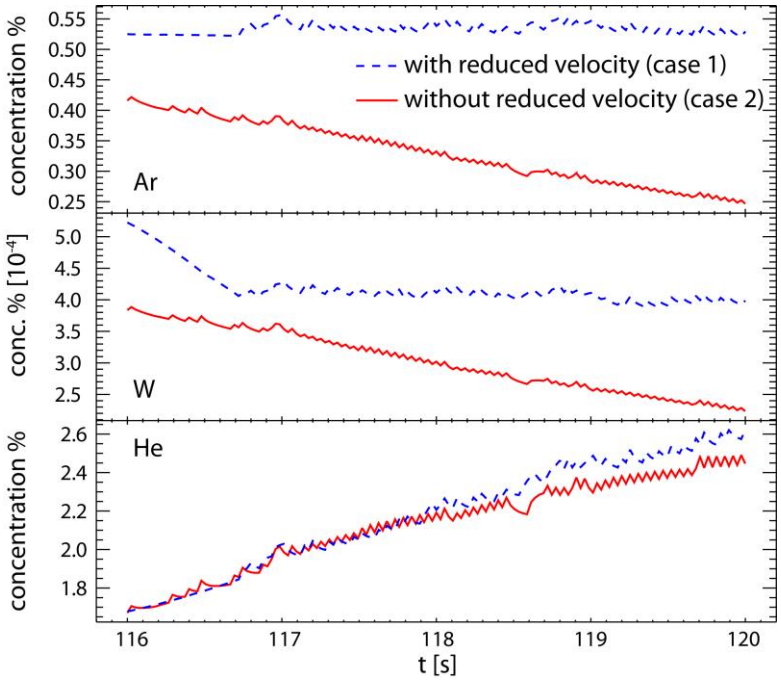

Figure 2. Ar, W and He concentration in the two simulated cases: higher Ar and W particle content (with reduced Ar and W escape velocity, dotted line) and lower Ar and W particle content (without reduced Ar and W escape velocity, solid line).

Figure 3 shows the neoclassical convective velocities for D (similar for T) and He, Ar, W impurities for case 1 (reduction in the escape velocities of Ar and W impurities). The velocity profiles of impurities are density weighted averages over the convective velocities for each ionisation stage. While Ar and W impurities are transported outwards in the ETB zone due to neoclassical convection, the neoclassical velocity for D and He is inwards directed. In case of no reduction in the escape velocities (case 2, not shown in the figure), an inward pinch of low Z particles (D, T and He) and an outward convection of higher Z impurities (Ar and W) are also present, but with slight variation of the velocities in absolute value.
The level of impurity concentration in these simulations is de facto imposed, as it mainly depends on initial and boundary conditions. In order to elaborate predictions for the impurity concentration levels, it would be necessary to carry out integrated simulations including the SOL and plasma-wall interaction which is out of the scope of this paper. The impurity concentrations obtained in these simulations correspond though to typical expectations for DEMO plasmas [19].

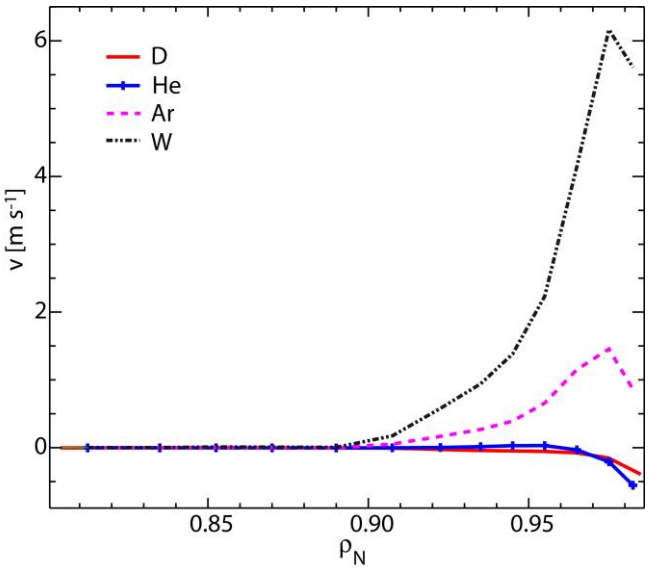

Figure 3. Neoclassical convective velocities for D (similar for T), He, Ar and W for case 1 (reduced escape velocities for Ar and W) at the end of the simulation shown in figure 2 (the profile is time averaged to avoid fluctuatons due to ELMs).

Neutral influx of D and T particles is adjusted by feedback to keep a line-average electron density of ~$8.5*10^{19}$ m^{-3} (corresponding to a volume-average density of ~$7.5*10^{19}$ m^{-3}). The influx is kept equal for D and T particles and needs to be in the order of >10^{23} s^{-1} to achieve the required density without pellet injection. Figure 4 shows neutral influx and the electron density in the two cases. In the simulated case with reduced escape velocity for high Z impurities (case 1), the neutral influx is almost halved. This is due to the increased high Z impurity density yielding increased outwards directed neoclassical high-Z impurity fluxes in the ETB due to temperature screening. These impurity fluxes are compensated by an increased inwards directed neoclassical flux of main ions that assists the fuelling by neutrals penetrating through the separatrix.
It can be concluded that a neoclassical inwards pinch for main ions may be present in the ETB in DEMO that significantly contributes to core fuelling and the maintenance of the core density in the presence of high Z impurities and large edge temperature gradients, while high Z impurities can be effectively screened from the core. Temperature screening may be detrimental for the removal of He from the core though, as the neoclassical pinch for He in the ETB is also predicted to be inwards directed due to the low Z value of He. In figure 3 the neoclassical convective velocity for He is indeed negative (i.e. inward directed) at the very edge of the plasma.
Increased impurity content causes increased radiation. This can be seen in figure 5, where the net power flowing through the separatrix (which takes into account also radiation losses) is closer to L-H transition power in the case with increased high Z impurity content due to the enhanced radiation. L-H transition power is here estimated by Martin scaling [26]. Despite the large fusion power, operation in H-mode might thus be marginal in terms of P_{net}/P_{L-H} which might affect plasma confinement provided that there is no hysteresis and the back transition power threshold P_{H-L} is close to or equal to P_{L-H} as observed in experiments [27]. This imposes an upper limit on the power that can be radiated by impurities to reduce the heat flux on the targets. Further investigations on this topic can be found in references [24],[19]. Fluctuations in P_{net} caused by uncontrolled ELMs might cause transient back transitions to L-mode in case of increased impurity radiation and further aggravate plasma confinement conditions.

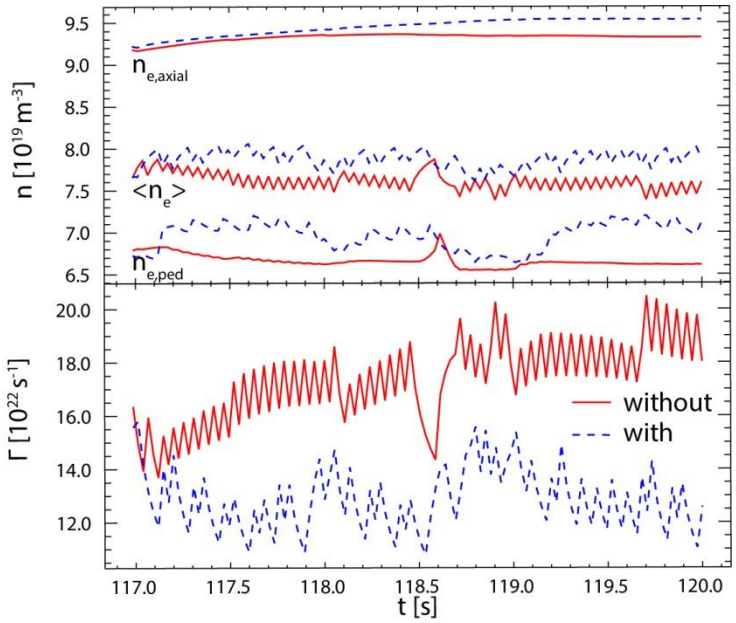

Figure 4. Electron density (at plasma centre, on average and pedestal - top) and D neutral influx (bottom), equal to the T neutral influx, at the separatrix for cases with (dotted line) or without (solid line) reduction of Ar and W escape velocities (higher and lower Ar and W particle content respectively).

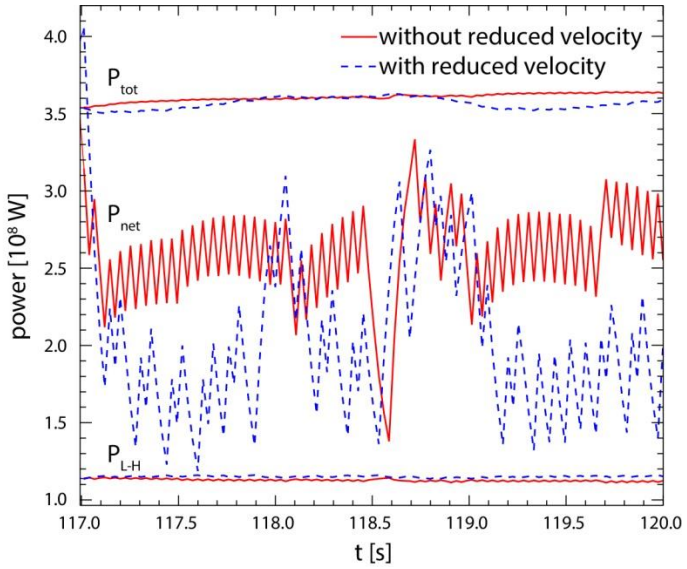

Figure 5. From top to bottom: total power, net power flowing through the separatrix, L-H power. Dotted line is with reduced Ar and W escape velocities (i.e. with increased impurity content), solid line is without. Fluctuations in P_{net} are caused by ELMs.

In both cases with high and low impurity content the target density can be reached and the temperature profile (not shown here) is kept almost unvaried, although with a very high prescibed neutral influx at the separatrix. The high content of He ash, which increases in time, might be a problem, while impurity contamination increase has a clear effect on radiation. Core accumulation of high Z impurities might be less of a concern, as these are predicted to be well screened from the core due to their abovementioned strong outwards directed neoclassical pinch in the ETB.

3.2 Scan in prescribed neutral influx at the separatrix

Gas puffing is an important fuelling tool for density control in present experiments, where the small dimension of SOL allows a significant neutral influx at the separatrix. In order to fuel the plasma, a particle must indeed travel from the wall to the separatrix without being ionized: considered the dimension and the large temperature gradient in DEMO, it is unlikely to have a large neutral influx at the separatrix. Regardless, a scan in the constant prescribed neutral influx at the separatrix has been performed, looking for the minimum flux to keep the desired core plasma density. Simulations here presented are started at t=120s of the reference case, i.e. the case without any reduction of Ar and W escape velocities shown in figure 4. Figure 6 illustrates the effect of different influxes on the electron density, plasma thermal energy and fusion power. Temporary oscillations in plasma conditions are caused by a sudden imposed variation of the neutral influx from a feedback controlled to a fixed value at t=120 s, when the scan in neutral influx is started. Temporary oscillations are also caused by the modification of local edge gradients caused by the variation of the neutral ionisation source that affects the ELM pattern.

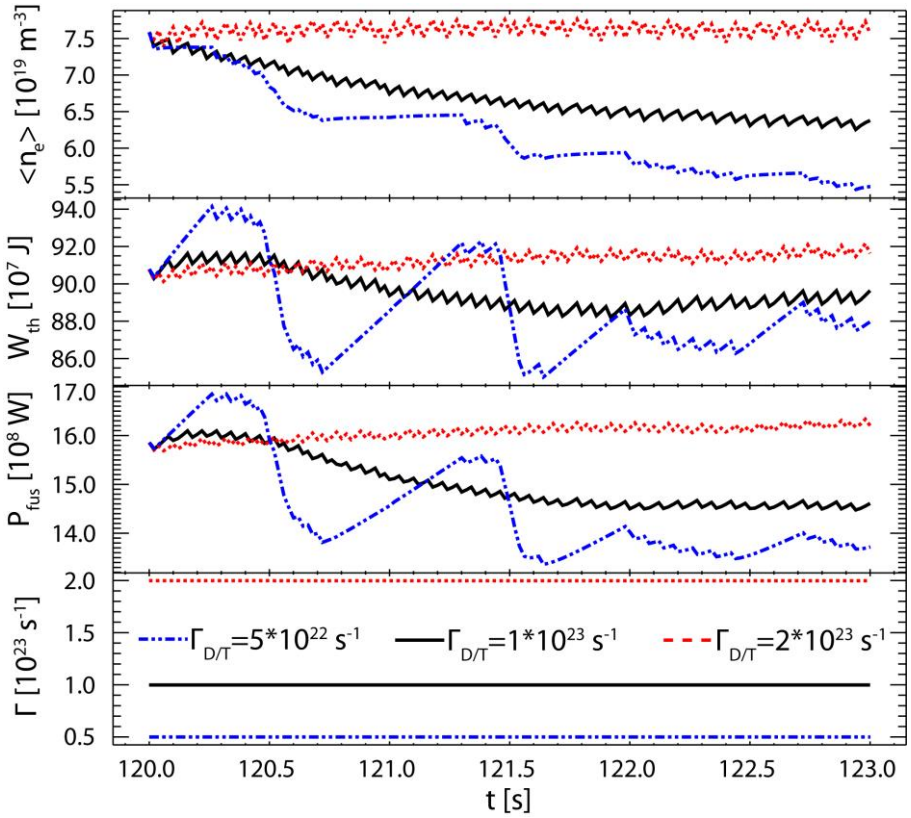

Figure 6. Effect of different neutral influxes at the separatrix on volume-average electron density, plasma thermal energy and fusion power. Fluxes of D or T are set to be equal (bottom plot).

A minimum of $4*10^{23}$ s^{-1} particle (D+T) influx is necessary to support the target DEMO scenario. This value seems to be very optimistic, probably making a gas puff only method unfeasible for DEMO. Also for ITER, gas puff is not expected to be suitable for core fuelling due to the efficient particle screening by the SOL [28], [29].
The present work has not analysed the real D-T throughput or pumping requirements, as an integrated core-SOL simulations would be necessary for that. However, as reported in this section, the neutral influx must be very large to maintain the core density only by gas puffing. Furthermore, most of injected gas particles will become completely ionised in the SOL, therefore the required externally applied gas puff rate should be orders of magnitude larger. Pumping capabilities will definitely not be able to cope with such large gas flux rates.

3.3 Scan in additional anomalous inward pinch in the ETB

Supposing the likely situation of almost all the neutrals ionizing in the SOL, and therefore negligible neutral influx at the separatrix, a scan in the additional anomalous inward pinch in the ETB has been performed. A more detailed discussion about the presence of anomalous pinch in the ETB can be found in reference [30].
Again, the aim here is to find the minimum value necessary to reach and maintain the target density. Figure 7 shows the result of this scan. The cases shown here starts at t=120s of the reference case, i.e. the case without any reduction of Ar and W escape velocities shown in figure 4. Divergences in plasma energy W_{th} and fusion power P_{fus} are caused by adaptation of pedestal conditions to the strong reduction of the neutral ionisation source (prescribed zero neutral flux at the separatrix for $t > 120$ s) and the application of an anomalous inwards pinch in the ETB, the latter yielding an increase in density on top of the pedestal. As a consequence of this increase, the temperature on top of the pedestal is reduced by ELMs to keep the maximum α in the ETB below α_{crit}. This reduction in temperature then propagates to the core due to profile stiffness. In addition to these effects, the core density starts to decrease in cases with lower anomalous inwards pinch, which also influences W_{th} and P_{fus}. The minimum additional velocity of D and T entering the plasma is ~2 m/s to achieve the reference density, although density cannot be controlled. A value of 2 m/s might be in the upper range of expectations for an anomalous pinch [30].

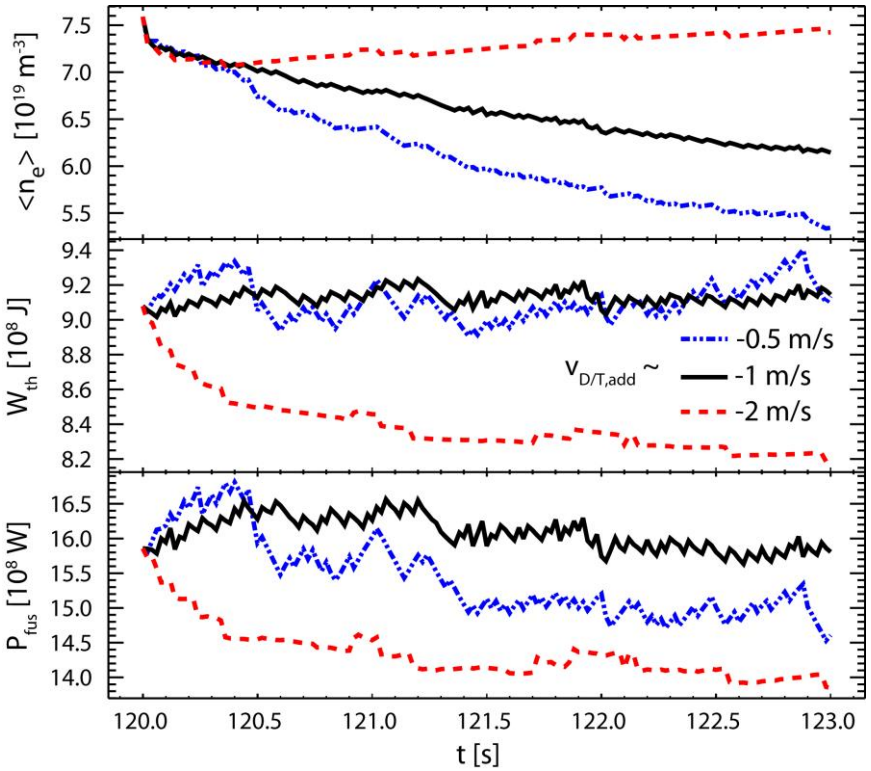

Figure 7. Scan in additional anomalous inward pinch in the ETB and consequent effects on volume-average density (top), plasma thermal energy (middle) and fusion power (bottom).

In addition to the scan here presented, and considering that gas puff-only option is likely to be not feasible for DEMO, we investigated if a certain level of inwards pinch combined with gas puffing can sustain the target density. We made a scan of the additional inwards pinch looking for the minimum value of neutral influx at the separatrix to sustain the target density. We found that the required neutral influx at the separatrix with values of inwards pinches below a certain threshold (~1.0 m/s in the case with reduced escape velocities for Ar and W, ~2.0 m/s in the case without any reduction in the escape velocities – cases of subsection 3.1) is still extremely large – at least two orders of magnitude more than what expected for ITER [28], [29]; while above this pinch threshold the neutral influx at the separatrix is not needed at all. Therefore fuelling by gas puff, even considering some level of inwards pinch, is likely to be not considerable as a possible actuator for core density control in DEMO during the high performance burning phase.

3.4 Scan in the target density at the top of the pedestal with pellet injection

Together with gas puffing, pellet injection is the most commonly used plasma fuelling method. The advantage of using pellets is the possibility to make the D and T particles ionize directly in the confined plasma, avoiding premature losses in the SOL, as happening for gas puff. The problem is to ensure a sufficient particle penetration towards the core, given the large temperature gradient characterizing DEMO pedestal. The aim of this scan is therefore to check the feasibility of keeping the target density by means of only pellet injection (from HFS). In the JETTO code a feedback control cycle is used to adjust rapidly the discrete particle source (pellets) in order to match the prescribed electron density at the top of the plasma pedestal. The controller compares the actual electron density on the top of the pedestal in the simulation with the prescribed one, and injects a pellet if the actual value is lower than the imposed one. Figure 8 depicts density, plasma thermal energy and fusion power for different target density at the top of the transport barrier. Oscillations in the global quantities shown in figure 8 are due also to ELMs in addition to pellet injection. The scan starts at t=120s of the reference case, i.e. the case without any reduction of Ar and W escape velocities shown in figure 4. ITER standard size pellets are used in this simulation, i.e. D-T ratio of 1:1, cylindrical pellet with height and diameter of 5 mm ($6.15*10^{21}$ particles per pellet). Injection speed is 500 m/s from the high field side (HFS) of the torus. Trajectory is calculated from pellets coordinates outside the plasma, which are R=5.03002m, Z=0.42336m and an injection angle of -0.1416 rad. The pellet injection

angle is defined as the angle between the direction of the pellet and the horizontal outward direction (i.e. towards the low field side of the tokamak). Neutral influx and additional inward pinch are here set to zero.

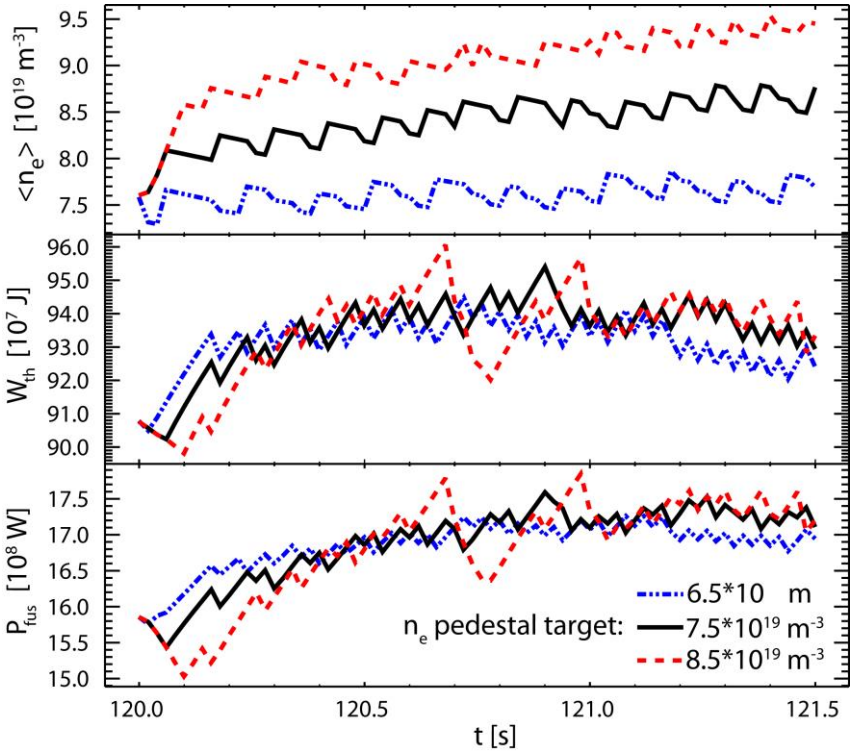

Figure 8. Scan in target electron density at the top of the pedestal and consequent volume-average electron density (top), plasma thermal energy (middle) and fusion power (bottom).

Because of the presence of the grad-B drift which leads the ExB drift of the ionized pellet particles towards the low field side (LFS), pellets have to be shot from the high field side (HFS) of the machine in order to make them penetrate beyond the plasma pedestal.
Particle penetration seems here not to be a problem, as figure 9 illustrates. Plasma fuelling is indeed achieved by an adequate pellet injection. The temperature is slightly affected by the increase target density at the top of the barrier (figure 9): since pellets penetrate significantly, the temperature is decreased by the larger number of injected particles. A key role in the efficacy of pellet fuelling is played by the ***E***x***B*** drift, which lets the ionized pellet particle to be deposited in a wider area. The next subsection clarifies the importance of this effect.

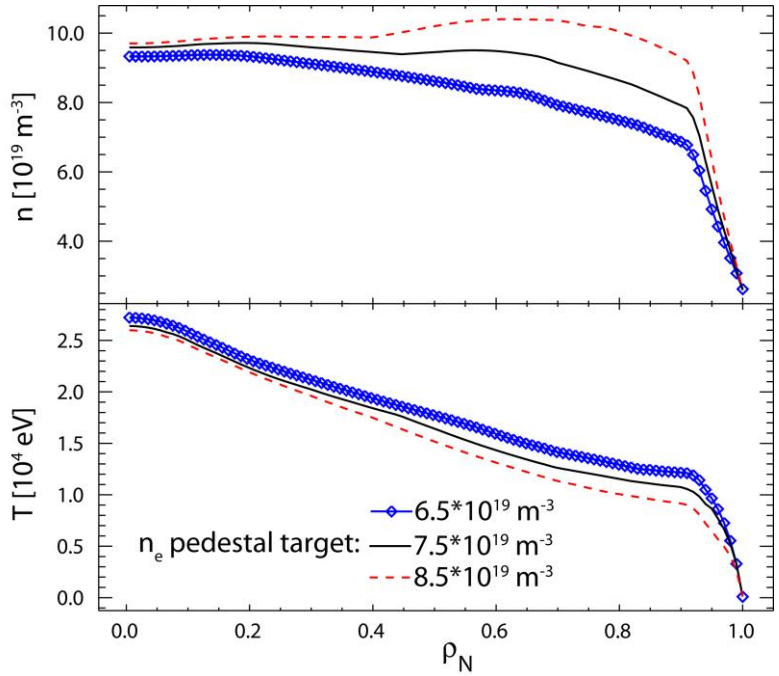

Figure 9. Electron density (top) and temperature (bottom) profiles during pellet injection with different targets of density at the top of the pedestal at t=121.3s (stationary conditions not yet reached in the core for higher n_e pedestal targets).

*3.4.1 Variation in the predicted **E**x**B** plasmoid drift*

The effect of the plasmoid ***E***x***B*** drift is critical to permit an efficient pellet core fuelling. Without this phenomenon and given the large temperature gradient in the plasma edge, the pellet ablates in a narrow outer zone and particles would be deposited only at the very edge of the plasma. Thanks to the drift, the zone where the pellet particles are finally deposited is considerably widened allowing them to penetrate deeper. This effect is illustrated in figure 10, where electron temperature and density are shown in the cases of presence and artificially imposed absence of the drift. Particle penetration and core fuelling is therefore strongly dependent on drift, as highlighted also for ITER [18],[31],[32].

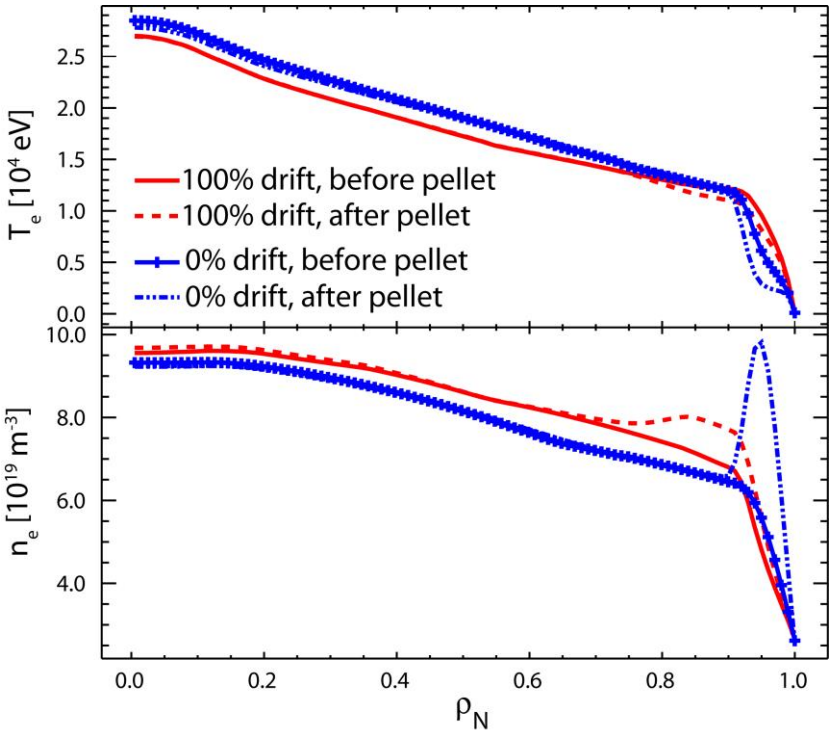

Figure 10. Effect of no ***E***x***B*** drift with respect to predicted case (100% drift) on temperature (top) and density (bottom) before and after pellet ablation at t~122s.

4. Effect of the pellet mass, pellet speed and injection geometry

In order to perform a preliminary assessment of the effect of varying the pellet mass, speed and injection geometry on the fuelling requirements for a typical DEMO scenario, we performed a series of runs similar to those presented in [18] for ITER. In particular, given the heat source profile, we chose an analytical expression of the form $\chi_{i,e}(\rho)=(\chi_{i,e}(0)-\chi_{i,e}(a))\rho^3+\chi(a)$ for the ion and electron heat conductivity profiles and tuned the coefficients in order to obtain a shape of the ion and electron temperature profiles similar to the one used in the nominal scenario. Subsequently, we assumed for the following simulations $\chi_e/D=4$ in the plasma core, where D is the main ion particle diffusivity (in reasonable agreement with values observed in present day tokamaks), $\chi_e=\chi_i=1.75$ m^2/s and $\chi_e/D=1.75$ in the pedestal (to obtain the right temperature and density pedestal height and to mimic the average effect of the ELMs to limit the pressure gradient in the pedestal). Finally, we introduced an anomalous inward pinch velocity $v_{inw}=0.5*D*r/a^2$ to allow for a degree of density peaking similar to the one predicted by more sophisticated physics based models, like, for example, GLF-23. The impurity concentration was not evolved, the Z_{eff} profile was assumed flat and equal to 2.2 and the radiated power profile was prescribed in order to obtain a steady state balance between alpha particles and neutral beam heating and conducted and radiated power losses. This reduces to the assumption that it was possible to maintain a concentration of the main radiating impurity (Ar in this case) compatible with the prescribed energy balance. Finally, we assumed that the only particle source was represented by the pellet deposition as prescribed by HPI2 code and implemented a feed-back scheme whereby a pellet was injected every time the volume average electron density dropped below 10^{20} m^{-3}. We assumed a 1:1 D-T pellet composition. Under these simulation conditions, we varied the plasma mass from $4*10^{21}$ to $13*10^{21}$ atoms, pellet speed from 300 m/s to 1000 m/s and injection geometry from vertical high field side (VHFS, aiming at the plasma magnetic axis form the high field side of the vacuum vessel with an injection angle close to 45°) to high field side (HFS, aiming at the plasma magnetic axis from the high field side of the vacuum vessel with an injection angle close to 3°). The duration of each run was 20 s, to allow the plasma to reach steady-state conditions.

The results are summarized in table 2, where, for each case, we show the pellet frequency required to maintain a stationary volume averaged plasma density close to 10^{20} m^{-3}. It can be seen that, for the same pellet mass and speed, HFS injection is more efficient than VHFS and the required pellet injection frequency increases from 2.6 Hz to 3.6 Hz when one moves from HFS to VHFS injection geometry. However, VHFS injection geometry allows higher pellet injection speed, because of the gentler curvature radius of the pellet

guide tube. Increasing the pellet speed from 300 m/s to 1000 m/s from the VHFS and keeping the pellet mass $4*10^{21}$ atoms results in a decrease of the required pellet injection frequency back to the original value of 2.6 Hz. However, the biggest reduction in required frequency (from 3.2 Hz to 1.0 Hz) is obtained by increasing the pellet mass by from $4*10^{21}$ to $13*10^{21}$ atoms. On one side, this is not surprising, since the particle throughput per pellet is multiplied by a factor of three, but, on the other side, it indicates that the pellet retention time (i. e. the time during which an amount of particle equal to the pellet mass is lost from the plasma) does not depend on the pellet mass.

This can be understood from figure 11, where we plot the pellet deposition profiles for the four cases of table 2. It can be seen that the peak of the pellet deposition profile predicted by HPI2 sits around ρ_N~0.85 and its location does not change significantly from one case to the other. The position of the peak represents the depth of the particle source, on which the pellet retention time depends [9]. This is due to the fact that, in DEMO, because of the height of the temperature pedestal (~10 keV) and of the steep temperature gradient inside it, the distance along which the pellet evaporates (ablation depth) is significantly shorter than the distance along which the pellet material is redistributed by the fast transport mechanism driven by the ∇B drift [33] (deposition depth). The latter distance depends mainly on the target plasma parameters and is likely to be similar for similar target plasmas.

From the simulations it is seen that more than 90% of the pellet particles are on average ablated at ρ_N>~0.95, while more than 90% of pellet particles are finally deposited at ρ_N>~0.7, with only small deviations for each case. Due to the very peripheral ablation, ELMs can be triggered by pellets, as suggested in reference [34]. However this topic has not been investigated here, being out of the scope of the present work and requiring the use of more complex models (e.g. as described in [34]).

The required influx of particles (particles per second) by gas puffing with respect to pellets in order to reach the same plasma condition differs of one order of magnitude, being $4*10^{23}$ s^{-1} for gas puff and between 1.0 and $1.4*10^{22}$ s^{-1} for pellet injection, the latter depending on pellet and injection parameters. This comparison shows that pellet injection is also a more efficient method to fuel the plasma.

The relatively narrow scan presented in this paper is being expanded to analyse in more detail the variations in the required pellet frequency with different pellet injection parameters. It should also be noted that any particular injection scheme should involve the analysis of the plasma response to the pellet perturbation in terms of both changes in transport and confinement properties and MHD stability. This analysis however is beyond the scope of this paper.

Table 2. Pellet injection frequency required to maintain a volume average density of 10^{20} m^{-3} for different pellet fuelling parameters.

Track	Mass (10^{21} D atoms)	Speed (m/s)	Frequency (Hz)
HFS	4	300	2.6
VHFS	4	300	3.2
VHFS	4	1000	2.6
VHFS	13	300	1.0

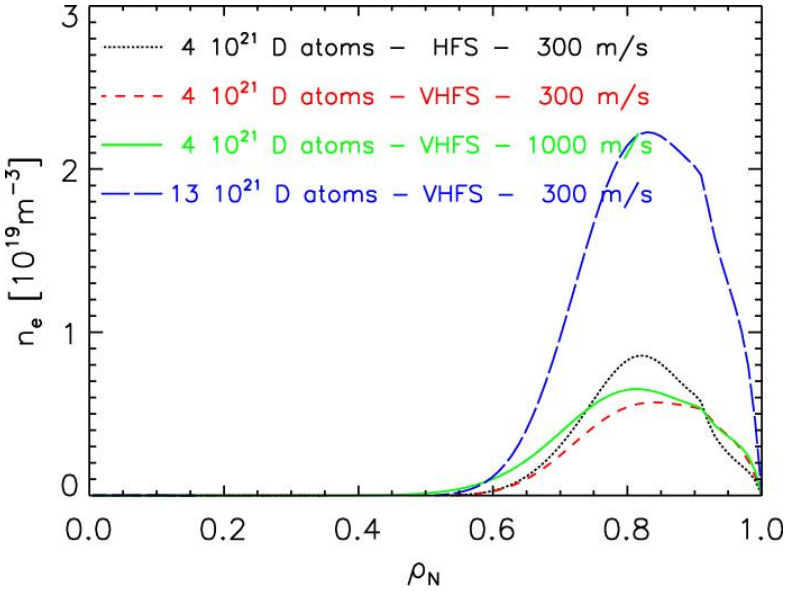

Figure 11. Pellet deposition profiles predicted by HPI2 code for the four cases described in table 2.

5. Conclusions

This work has investigated the density control issue for DEMO inductive scenario, analysing the effects of different direct and indirect density actuators. The DEMO scenario at high fusion performance imposes strict limits on density and temperature profiles. Fusion power exceeding 1500 MW may be achieved only with optimistic assumption of pedestal pressure (about 220 kPa at the top of the pedestal, double than ITER prediction). A line-average density of ~$8.0*10^{19}$ m^{-3} can only be maintained (with given boundary conditions) if an extremely high D+T neutral influx at the separatrix could be achieved only by gas puff. Given the large temperature gradient in the edge, core density control via gas puff might be impossible. With zero neutral influx at the separatrix, i.e. complete ionisation in the SOL, a similar density level could only be obtained (but not controlled) with a large hypothetical anomalous inwards pinch in the ETB of more than 2 m/s. There may indeed be a neoclassical inwards pinch for the main ions, although typically < ~1.0 m/s, compensating a large outward convection for impurities due to temperature screening. This effect may thus be helpful not only for the control of the core contamination by high Z impurities but also to partly fuel the plasma by an inward directed neoclassical main ion pinch. Even considering a milder inwards pinch in the order of < ~1.0 m/s, the required neutral influx at the separatrix remains extremely large, confirming that gas puff option is probably not feasible for DEMO fuelling. Control of He ash contamination in the core might become a problem due to very high fusion power. He particle content is indeed increasing during the simulated interval. Pellet injection could represent a solution both for D:T ratio and density control. Stationary H-mode at large densities seems to be achievable and controllable by pellet injection in the order of ~500 m/s from the HFS (with low injection angle), as shown by simulations presented in subsection 3.4. Other solutions may be considered, as higher velocity from the VHFS (vertical HFS, with high 45° injection angle) or higher pellet mass, in order to reduce the pellet injection frequency. Given the very unfavourable ablation condition, pellet fuelling efficiency is entirely determined by the plasmoid $\boldsymbol{E}x\boldsymbol{B}$ drift which is critical for core fuelling. Injection from HFS is the solution adopted also for ITER, due to the higher pellet penetration. Maximum pellet injection speed for ITER is expected to be 300 m/s, but injection systems with higher speeds have been tested [35], [36].

In conclusion, given the predicted transport level and plasma conditions, pellet injection might be the only particle source assuring a reliable density control at level required for high fusion performance of DEMO scenario. Impurity core contamination is a critical subject, especially considering the large amount of He ash created by fusion processes.

Acknowledgments

This project has received funding from the European Union's Horizon 2020 research and innovation programme under grant agreement number 633053. The views and opinions expressed herein do not necessarily reflect those of the European Commission. One of the authors (PV) gratefully acknowledges the hospitality of the Atominstitut (ATI), Vienna, during his visit.

References

[1] Romanelli F *et al* Fusion Electricity - A roadmap to the realisation of fusion energy ISBN 978-3-00-040720-8
[2] Sakamoto R *et al* 2012 *Nucl. Fusion* **52** 083006
[3] Mukhovatov V *et al* 2007 *Nucl. Fusion* **47** S404
[4] Romanelli M *et al* 2014 *Plasma and Fusion Research* **9** 3403023
[5] Zagórski R *et al* 2013 *Nucl. Fusion* **53** 073030
[6] Stankiewicz R and Stępniewski W 2014 *Contributions to Plasma Physics* **54** 358
[7] Zohm H *et al* 2013 *Nucl. Fusion* **53** 073019
[8] Belo P *et al* 2004 *Plasma Phys. Control. Fusion* **46** 1299
[9] Valovič M *et al* 2008 *Nucl. Fusion* **48** 075006
[10] Federici G *et al* 2013 *Fusion Engineering (SOFE)*, 2013 1-8 IEEE 25th Symposium on Fusion Engineering
[11] Cenacchi G and Taroni A 1988 Rapporto ENEA RT/TIB(88)5
[12] Lauro-Taroni L *et al* 1994 *Proceedings 21st EPS Conference Controlled Fusion and Plasma Physics*
[13] Strachan J D *et al* 2011 *J. Nucl. Mater.* **415** S501
[14] Giroud C *et al* 2007 *Nucl. Fus.* **47** 313
[15] Waltz R E 1997 *Phys. Plasmas* **4** 2482
[16] Houlberg W *et al* 1997 *Phys. Plasmas* **4** 3230
[17] Pereverzev G V and Corrigan G 2008 *Comp. Phys. Comm.* **179** 579-585
[18] Garzotti L *et al* 2012 *Nucl. Fusion* **52** 013002
[19] Wenninger R P *et al* 2014 *Nucl. Fusion* **54** 114003
[20] Challis C D *et al* 1989 *Nucl. Fusion* **29** 563
[21] Pégourié B *et al* 2007 *Nucl. Fusion* **47** 44
[22] Pacher H D *et al* 2011 *J. Nucl. Mater.* **415** S492
[23] Doyle E J *et al* Progress in the ITER Physics Basis Chapter 2: Plasma confinement and transport 2007 Nucl. Fusion **47** S18
[24] Wenninger R *et al* 2015 *Nucl. Fusion* **55** 063003
[25] Hirshman S P and Sigmar D J 1981 *Nucl. Fusion* **21** 1079
[26] Martin Y R *et al* 2008 Journal of Physics: Conference Series **123** 012033
[27] Maggi C F *et al*, Proc. 40th EPS Conf. on Plasma Physics (Espoo, Finland, 2013), [P2.168]
[28] Kukushkin A S *et al* 2011 *J. Nucl. Mater.* **415** S497
[29] Romanelli M *et al* "Modelling of Plasma Performance and Transient Density Behaviour in the H-mode access for ITER Gas Fuelled Scenarios", accepted for publication in *Nucl. Fusion*
[30] Willensdorfer M *et al* 2013 *Nucl. Fusion* **53** 093020
[31] Parail V *et al* 2009 *Nucl. Fusion* **49** 075030
[32] Pegourie B *et al* 2009 *Plasma Phys. Control. Fusion* **51** 124023
[33] Rozhansky V *et al* 1995 *Plasma Phys. Control. Fusion* **37** 399
[34] Hayashi N *et al* 2011 *Nucl. Fusion* **51** 103030
[35] A Loarte *et al* Progress in the ITER Physics Basis Chapter 4: Power and particle control 2007 Nucl. Fusion **47** S203
[36] Maruyama S *et al* 2012 *Proc. 24th Int. Conf. on Fusion Energy (San Diego, 2012)[ITR/P5-24] http://www-naweb.iaea.org/napc/physics/FEC/FEC2012/index.htm*